Skyrmion dynamics in chiral ferromagnets under spin-transfer torque

Stavros Komineas[1] and Nikos Papanicolaou[2]
[1]*Department of Mathematics and Applied Mathematics, University of Crete, 71003 Heraklion, Crete, Greece*
[2]*Department of Physics, University of Crete, 71003 Heraklion, Crete, Greece*

(Received 22 August 2015; revised manuscript received 21 October 2015; published 6 November 2015)

We study the dynamics of skyrmions under spin-transfer torque in Dzyaloshinskii-Moriya materials with easy-axis anisotropy. In particular, we study the motion of a topological skyrmion with skyrmion number $Q = 1$ and a nontopological skyrmionium with $Q = 0$ using their linear momentum, virial relations, and numerical simulations. The nontopological $Q = 0$ skyrmionium is accelerated in the direction of the current flow and it either reaches a steady state with constant velocity, or it is elongated to infinity. The steady-state velocity is given by a balance between current and dissipation and has an upper limit. In contrast, the topological $Q = 1$ skyrmion converges to a steady state with constant velocity at an angle to the current flow. When the spin current stops the $Q = 1$ skyrmion is spontaneously pinned, whereas the $Q = 0$ skyrmionium continues propagation. Exact solutions for the propagating skyrmionium are identified as solutions of equations given numerically in a previous work. Further exact results for propagating skyrmions are given in the case of the pure exchange model. The traveling solutions provide arguments that a spin-polarized current will cause rigid motion of a skyrmion or a skyrmionium.

DOI: 10.1103/PhysRevB.92.174405 PACS number(s): 75.78.−n, 75.76.+j, 75.78.Fg

I. INTRODUCTION

Soliton structures are found in ferromagnets and they can be considered as an encoding of magnetic information which is robust both under temperature and external probes. Stable topological solitons with the structure of a skyrmion had been predicted in the presence of the Dzyaloshinskii-Moriya (DM) interaction [1,2] and they were observed in recent years as isolated structures [3,4] or forming lattices [5–7]. In the presence of easy-axis anisotropy there are topological skyrmions with skyrmion number $Q = 1$ as well as nontopological $Q = 0$ solitons (2π vortices) [8] and related equilibrium states in confined magnetic elements [9].

Skyrmions could be the stable and robust entities that are needed for the technology of recording and transferring information, currently mainly obtained in magnetic media using domain walls [10]. The propagation of magnetic information is done most conveniently by the injection of electrical spin-polarized current. Single skyrmions and skyrmion lattices can be set in motion suggesting a promising technique for the manipulation of magnetic information [11–17]. Propagation of skyrmions by spin current or the related spin-Hall effect may be a promising strategy for the implementation of racetrack memories [18].

The existence of two species of skyrmions ($Q = 0$ and $Q \neq 0$) has allowed theoretical predictions for dramatically different dynamical behaviors [19]. We show here that spin torque accelerates a $Q = 0$ skyrmionium and we describe the process theoretically, while the study is complemented by numerical simulations. The skyrmionium may reach a steady state or it may absorb energy from the current and expand without limit. A skyrmionium propagating even when the external probe is switched off can be obtained. The situation is contrasted to the more well-studied case of a $Q = 1$ skyrmion under spin torque.

The outline of the paper is the following. Section II gives a description of the Landau-Lifshitz model including damping and spin-transfer torques and provides the main theoretical tools. Section III is on the dynamics of a $Q = 0$ skyrmionium and Sec. IV is on the dynamics of a $Q = 1$ skyrmion. Section V contains our concluding remarks. An Appendix gives analytical results on the pure exchange model.

II. MAGNETIZATION DYNAMICS UNDER SPIN-TRANSFER TORQUE

We assume a thin ferromagnetic film with a Dzyaloshinksii-Moriya (DM) interaction. Let $\boldsymbol{M}(x,y,t)$ be the magnetization vector with M_s the saturation magnetization and define the normalized magnetization $\boldsymbol{m} = \boldsymbol{M}/M_s$, so that $\boldsymbol{m}^2 = 1$. The conservative Landau-Lifshitz (LL) equation for the statics and dynamics of the magnetization is

$$\partial_t \boldsymbol{m} = -\boldsymbol{m} \times \boldsymbol{f} \tag{1}$$

and is valid in the absence of damping and external probes. We consider an effective field $\boldsymbol{f}$ which includes an exchange interaction with constant A, an easy-axis anisotropy perpendicular to the (x_1,x_2) plane of the film with constant K, and a DM interaction with constant D [2]. If the energy is W then the effective field $\boldsymbol{f} = -\delta W/\delta \boldsymbol{m}$ is

$$\begin{aligned}\mathbf{f} &= \Delta \mathbf{m} + \kappa\, m_3 \hat{\mathbf{e}}_3 \\ &\quad - 2\lambda\, [\partial_2 m_3\, \hat{\mathbf{e}}_1 - \partial_1 m_3\, \hat{\mathbf{e}}_2 + (\partial_1 m_2 - \partial_2 m_1)\, \hat{\mathbf{e}}_3],\end{aligned} \tag{2}$$

where we have used $\ell_{\rm D} = 2A/|D|$ as the unit of length. The parameter

$$\kappa \equiv \frac{K}{K_0}, \quad K_0 = \frac{D^2}{4A} \tag{3}$$

is the rationalized (dimensionless) anisotropy constant and $\lambda = D/|D| = \pm 1$ will be referred to as the chirality. We choose chirality $\lambda = 1$ in all of our numerical calculations, while κ is taken to be positive (easy-axis anisotropy). We have not included the demagnetizing field in Eq. (2) because it does not affect skyrmion configurations in a qualitatively significant way [20]; it introduces a dependence of the skyrmion size on the film thickness [21]. The time variable t in Eq. (4) is measured in units of $\tau_0 = 2AM_s/(\gamma D^2)$, where γ is the gyromagnetic ratio.

When a spin-polarized current is flowing in the plane of the film, say, in the x_1 direction, and we also include damping effects, the magnetization obeys the Landau-Lifshitz-Gilbert equation with two additional terms for the spin-transfer torque [22–24]:

$$(\partial_t + u\,\partial_1)\boldsymbol{m} = -\boldsymbol{m}\times\boldsymbol{f} + \boldsymbol{m}\times(\alpha\partial_t + \beta u\,\partial_1)\boldsymbol{m}. \quad (4)$$

The dissipation constant is α, while u is the effective spin velocity parallel to the spin current and β is the nonadiabatic spin-transfer torque parameter.

In the absence of spin torque, that is, for $u = 0$ the ground state of the model is the *spiral state* for sufficiently small anisotropy. For $\kappa > \kappa_c = \pi^2/4 \approx 2.4674$ the ground state is either of the two uniform ferromagnetic states $\boldsymbol{m} = (0,0,\pm 1)$. In the latter case, skyrmions are excited states and they are classified by the skyrmion number defined as

$$Q = \frac{1}{4\pi}\int q\,d^2x, \quad q = \frac{1}{2}\epsilon_{\mu\nu}\mathbf{m}\cdot(\partial_\nu\mathbf{m}\times\partial_\mu\mathbf{m}), \quad (5)$$

where q is called the *topological density*. The skyrmion number Q is integer-valued ($Q = 0,\pm 1,\pm 2,\ldots$) for all magnetic configurations such that $\mathbf{m} = (0,0,\pm 1)$ at spatial infinity. For definiteness we will assume $\mathbf{m} = (0,0,1)$ in all our calculations.

Axially symmetric skyrmion configurations are conveniently described in terms of the standard spherical parametrization given by

$$m_1 = \sin\Theta\cos\Phi, \quad m_2 = \sin\Theta\sin\Phi, \quad m_3 = \cos\Theta \quad (6)$$

with the ansatz

$$\Theta = \theta(\rho), \quad \Phi = \phi + \pi/2, \quad (7)$$

where (ρ,ϕ) are polar coordinates. Solving Eq. (1) with boundary conditions $\theta(\rho = 0) = \pi$ and $\theta(\rho\to\infty) = 0$ leads to a static skyrmion with $Q = 1$ shown in Fig. 1. If the boundary conditions are $\theta(\rho = 0) = 2\pi, \theta(\rho\to\infty) = 0$ a $Q = 0$ configuration is found [8], which has been called a "skyrmionium" [19,25] and is shown in Fig. 2.

Equation (4) can be written in the form

$$\begin{aligned}\partial_t\boldsymbol{m} &= -\boldsymbol{m}\times\boldsymbol{g},\\ \boldsymbol{g} &= \frac{1}{1+\alpha^2}[\boldsymbol{f} + \alpha\,\boldsymbol{m}\times\boldsymbol{f} - (\beta-\alpha)u\,\partial_1\boldsymbol{m}\\ &\quad -\alpha(\beta-\alpha)u\,\boldsymbol{m}\times\partial_1\boldsymbol{m}].\end{aligned} \quad (8)$$

The time derivative of the topological density is

$$\dot{q} = -\epsilon_{\mu\nu}\,\partial_\mu(\boldsymbol{g}\cdot\partial_\nu\boldsymbol{m}) \quad (9)$$

as can be found by a straightforward calculation. We now define the moments of the topological density

$$I_\mu = \int x_\mu q\,d^2x, \quad \mu = 1,2 \quad (10)$$

and we have the fundamental result that these are conserved quantities, i.e., $\dot{I}_\mu = 0$, within the conservative Eq. (1) in an infinite film [26,27]. For the proof we set $\boldsymbol{g} = \boldsymbol{f}$ in Eq. (9) and the details for the specific $\boldsymbol{f}$ of Eq. (2) are given in Ref. [19].

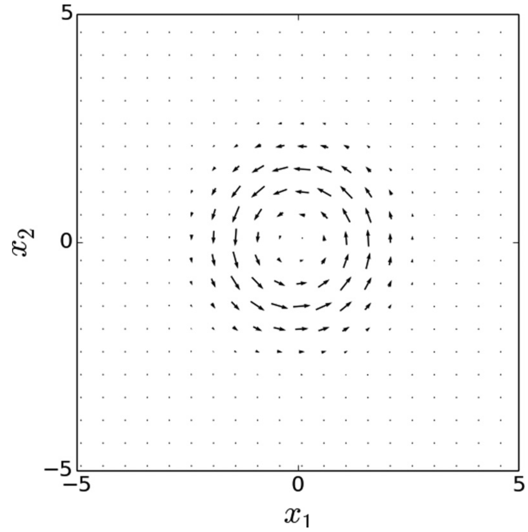

FIG. 1. Axially symmetric ($Q = 1$) skyrmion represented through the projection (m_1,m_2) of the magnetization vector on the plane. It is calculated as a static solution of Eq. (1) for anisotropy $\kappa = 3$.

The moments I_μ are no longer conserved within Eq. (8) due to the damping and spin torque terms and we find

$$\begin{aligned}(1+\alpha^2)\dot{I}_1 &= -(\beta-\alpha)u\,d_{12} + \alpha\,D_2 + (1+\alpha\beta)u\,(4\pi Q),\\ (1+\alpha^2)\dot{I}_2 &= (\beta-\alpha)u\,d_{11} - \alpha\,D_1,\end{aligned} \quad (11)$$

where we have used the notation

$$\begin{aligned}d_{\mu\nu} &= \int(\partial_\mu\boldsymbol{m}\cdot\partial_\nu\boldsymbol{m})\,d^2x, \quad \mu,\nu = 1,2,\\ D_\mu &= \int(\boldsymbol{m}\times\boldsymbol{f})\cdot\partial_\mu\boldsymbol{m}\,d^2x.\end{aligned} \quad (12)$$

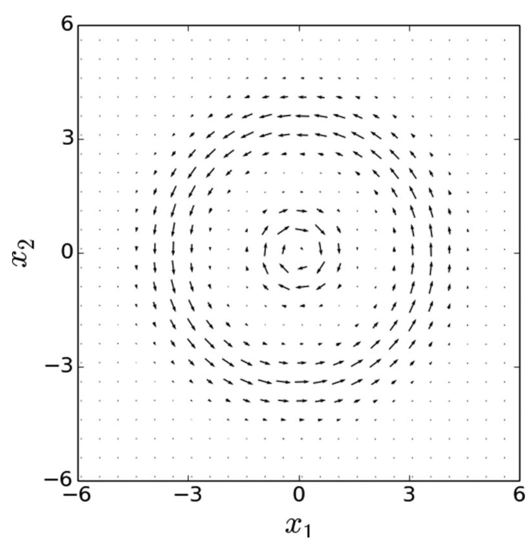

FIG. 2. Axially symmetric ($Q = 0$) skyrmionium represented through the projection (m_1,m_2) of the magnetization vector on the plane It is calculated as a static solution of Eq. (1) for anisotropy $\kappa = 3$.

Equations (11) give an explicit result since they may be applied for any magnetic configuration.

Let us consider a skyrmion which is initially static within the conservative LL Eq. (1) and we suddenly apply an electrical current according to Eq. (4). This will start to move and the overall motion is given by Eqs. (11). As a next step we will assume that it will eventually reach a steady state with velocity $\boldsymbol{v} = (v_1,v_2)$. We may then write the traveling wave ansatz for the magnetization

$$\begin{aligned} \boldsymbol{m}(x_1,x_2,t) &= \boldsymbol{m}_0(\xi_1,\xi_2;v_1,v_2), \\ \xi_1 \equiv x_1 - v_1 t, &\quad \xi_2 = x_2 - v_2 t \end{aligned} \tag{13}$$

so that $\partial_t \boldsymbol{m} = -v_\nu \partial_\nu \boldsymbol{m}$ with $\nu = 1,2$. Inserting this in Eq. (4) we obtain

$$u\,\partial_1 \boldsymbol{m} - v_\nu \partial_\nu \boldsymbol{m} = -\boldsymbol{m} \times \boldsymbol{f} + \boldsymbol{m} \times (\beta\,u\,\partial_1 \boldsymbol{m} - \alpha v_\nu\,\partial_\nu \boldsymbol{m}). \tag{14}$$

We will assume that ∂_1,∂_2 in the above equation denote derivatives with respect to ξ_1,ξ_2.

We may now take the cross product of both sides in Eq. (14) with $\partial_\mu \boldsymbol{m}$ for $\mu = 1$ or 2 and then contract with $\boldsymbol{m}$. In the result, the term containing the effective field $\boldsymbol{f}$ (i.e., the term due to the conservative part of the equation) is written as a total derivative [26,27]:

$$-\boldsymbol{f} \cdot \partial_\mu \boldsymbol{m} = \partial_\nu \sigma_{\mu\nu}, \tag{15}$$

where the explicit form of the tensor $\sigma_{\mu\nu}$ for the effective field (2) is given in Ref. [19]. Upon integrating over all space the total derivative (15) vanishes and we obtain the pair of virial relations [28,29]

$$\begin{aligned} (-4\pi Q + \alpha d_{21}) v_1 + \alpha d_{22} v_2 &= \beta u\, d_{21} - u\,(4\pi Q), \\ \alpha d_{11} v_1 + (4\pi Q + \alpha d_{12}) v_2 &= \beta u\, d_{11}. \end{aligned} \tag{16}$$

Some general conclusions can be drawn from Eqs. (11) and (16). The dynamics and the steady-state velocity (v_1,v_2) can be obtained in particular cases as will be discussed in the next sections for the cases of a skyrmionium and a skyrmion.

III. TRAVELING $Q = 0$ SKYRMIONIUM

Let us consider the $Q = 0$ skyrmionium of Fig. 2 which is a static solution of Eq. (1) and we suddenly apply a spin-polarized current. In order to follow how the initial skyrmionium will be accelerated we will follow its *linear momentum* which is defined via the conserved I_μ of Eq. (10) as [26,27]

$$P_\mu = \epsilon_{\mu\nu} I_\nu, \quad \mu,\nu = 1 \text{ or } 2. \tag{17}$$

To be sure, the above quantities have the meaning of a linear momentum within the Hamiltonian equations (1). We will though extend their use in the full model (4). The time derivatives of the components of the linear momentum are given by Eqs. (11) applied for $Q = 0$:

$$\begin{aligned} (1+\alpha^2)\dot{P}_1 &= (\beta - \alpha) u\, d_{11} - \alpha\, D_1, \\ (1+\alpha^2)\dot{P}_2 &= (\beta - \alpha) u\, d_{12} - \alpha\, D_2. \end{aligned} \tag{18}$$

These relations give a simple result when we apply them for the initial skyrmionium which is a static solution of Eq. (1) (thus $D_\mu = 0$) and is axially symmetric (thus $d_{12} = 0$). We obtain

$$\dot{P}_1 = \frac{\beta - \alpha}{1+\alpha^2} u\, d_{11}, \quad \dot{P}_2 = 0. \tag{19}$$

The skyrmionium is accelerated acquiring a linear momentum component along the x_1 direction only. The acceleration is zero when $\beta = \alpha$ and this point will be clarified in the following when we present solutions of Eq. (4).

If the skyrmionium eventually reaches a traveling steady state then the virial relations (16) apply. For $Q = 0$ they reduce to a simple form and give the velocity of the steady state:

$$\begin{pmatrix} d_{11} & d_{12} \\ d_{21} & d_{22} \end{pmatrix} \begin{pmatrix} \alpha v_1 - \beta u \\ \alpha v_2 \end{pmatrix} = \begin{pmatrix} 0 \\ 0 \end{pmatrix} \Rightarrow \begin{cases} v_1 & = \frac{\beta}{\alpha} u, \\ v_2 & = 0, \end{cases} \tag{20}$$

provided $\det(d_{\mu\nu}) \neq 0$. Therefore, the skyrmionium in steady state moves in the direction of the current. The presence of dissipation is crucial as there is apparently no steady state for $\alpha = 0$. The acceleration process along the axis of the current described by Eqs. (19) is compatible with the steady-state velocity in Eq. (20).

We can find exact traveling solutions for a skyrmionium under spin-transfer torque. In order to show how this can be achieved, we start by considering the special case $\beta = \alpha$, for which Eq. (4) becomes

$$(\partial_t + u\,\partial_1)\boldsymbol{m} = -\boldsymbol{m} \times \boldsymbol{f} + \alpha\,\boldsymbol{m} \times (\partial_t + u\,\partial_1)\boldsymbol{m}. \tag{21}$$

We look for traveling wave solutions of the form (13) and we choose $v_1 = u$, $v_2 = 0$. We have $\partial_t \boldsymbol{m} = -u \partial_1 \boldsymbol{m}$, which is used to reduce Eq. (21) to $\boldsymbol{m} \times \boldsymbol{f} = 0$. Thus, if we choose $\boldsymbol{n}(x_1,x_2)$ to be a static solution of Eq. (1) then $\boldsymbol{m}(x_1,x_2,t) = \boldsymbol{n}(\xi_1,x_2)$ gives a configuration which satisfies Eq. (21) and is a traveling solution with velocity $(v_1,v_2) = (u,0)$. In conclusion, the static skyrmionium solution of the conservative LL Eq. (1) (shown in Fig. 2) is a traveling solution of the full equation (4) for the case $\beta = \alpha$. That also explains the vanishing acceleration in Eqs. (19). This mathematical result has the following physical content. If we apply spin-polarized current to an initially static skyrmionium this is expected to be set into rigid motion without significant deformations. The same can also be argued for the traveling skyrmion in the next section.

Let us now generalize the above for $\beta \neq \alpha$. The traveling wave ansatz (13) with the choice $(v_1,v_2) = (v,0)$ is used to reduce Eq. (4) to

$$(u - v)\partial_1 \boldsymbol{m} = -\boldsymbol{m} \times \boldsymbol{f} + (\beta u - \alpha v)\,\boldsymbol{m} \times \partial_1 \boldsymbol{m}. \tag{22}$$

We now choose $v = \beta u/\alpha$ and the equation is further reduced to

$$v_0\,\partial_1 \boldsymbol{m} = \boldsymbol{m} \times \boldsymbol{f}, \quad v_0 = \frac{\beta - \alpha}{\alpha} u. \tag{23}$$

This equation is identical to that for a steady-state traveling with a velocity v_0 within the conservative LL Eq. (1). Such states were numerically calculated and studied in Ref. [19]. A family of traveling skyrmioniums were found with velocities up to a critical velocity $v_c \approx 0.102$. In conclusion, if we denote the solutions of Eq. (23) by $\boldsymbol{n}(x_1,x_2;v_0)$ then the form $\boldsymbol{m}(x_1,x_2,t) = \boldsymbol{n}(\xi_1,x_2;v_0)$ with $\xi_1 = x_1 - vt$ is a traveling wave solution of Eq. (4) with velocity $v = \beta u/\alpha$. The condition $v_0 < v_c$ for the skyrmionium configuration

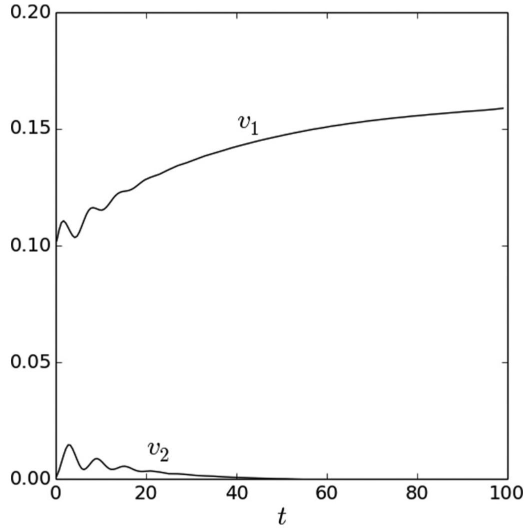

FIG. 3. Velocity components $(v_1,v_2) = (\dot{X}_1,\dot{X}_2)$ for a skyrmionium under spin torque with parameter values (25). The expected velocity at the steady state is $(v_1,v_2) = (0.167,0)$.

satisfying Eq. (23) becomes in the presence of spin-transfer torque

$$v < u + v_c. \tag{24}$$

We have conducted a numerical simulation using the parameter set

$$\alpha = 0.06, \quad u = 0.1, \quad \beta = 0.1. \tag{25}$$

We use as an initial condition the skyrmionium of Fig. 2 with $\kappa = 3$ and apply the spin current. The expected velocity in the steady state is given by Eq. (20) and is $v_1 = 0.167$, $v_2 = 0$. The prediction is confirmed by the numerical simulation. We define the position of the skyrmionium as (X_1,X_2) with

$$X_\mu = \frac{\int x_\mu (1-m_3)\, d^2x}{\int (1-m_3)\, d^2x}. \tag{26}$$

Figure 3 shows the velocity $(v_1,v_2) = (\dot{X}_1,\dot{X}_2)$ as a function of time. The skyrmionium is accelerated and the change of linear momentum at $t = 0$ verifies the prediction $\dot{P}_1 = 0.34$ calculated by Eq. (19) when we use the numerically calculated value $d_{11} = 57.1$. The velocity at $t = 0$ is $v_1(t = 0) \approx u = 0.1$ and it increases to $v_1(t = 100) = 0.16$ at the end of this simulation. The component v_2 acquires some small value at the initial stages of the simulation and it later goes to zero. The results have been confirmed also by a simulation in a moving frame, running for times longer than those shown Fig. 3, where it is seen that (v_1,v_2) converge to the expected values at the steady state.

Figure 4 shows two snapshots of the skyrmionium under spin torque. At the initial time $t = 0$ we have the axially symmetric static solution of Eq. (1). The accelerated skyrmionium at $t = 40$ has velocity $v_1 = 0.143$ and has lost axial symmetry: its central part has moved lower. It is very similar to the propagating skyrmionium studied in Ref. [19]. We conclude that the application of spin current is a method to obtain a propagating skyrmionium in a steady state. We note that the skyrmionium continues to travel at its acquired velocity when the spin current is switched off, irrespectively of whether a steady state was reached or not. This is in stark contrast to the dynamics of a skyrmion or to ordinary domain wall dynamics.

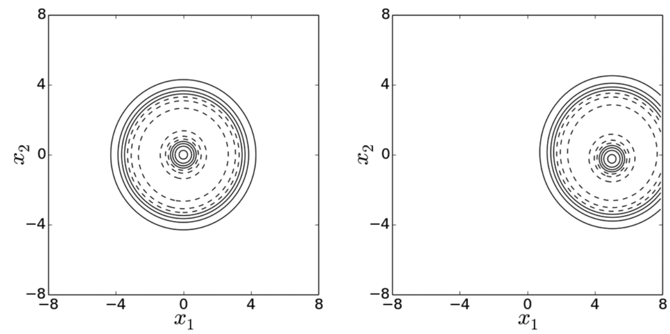

FIG. 4. Contour plots of m_3 for a skyrmionium under spin torque with parameter values (25). (Left) The initial condition, at $t = 0$, is a static skyrmionium solution of Eq. (1). (Right) The skyrmionium at $t = 40$ when it has been accelerated. The inner part has moved down relative to the outer part. The contour levels plotted are $m_3 = 0.9, 0.6, 0.3, 0.0$ (solid lines) and $m_3 = -0.3, -0.6, -0.9$ (dashed lines).

Let us now consider a second set of parameter values,

$$\alpha = 0.04, \quad u = 0.1, \quad \beta = 0.1, \tag{27}$$

which gives a velocity for the skyrmionium $v = \beta u/\alpha = 0.25$ violating condition (24). In this case the skyrmionium is accelerated until its velocity approaches the limiting value $u + v_c$ while the configuration becomes elongated along the x_2 axis and eventually reaches the boundaries of our numerical grid. Presumably, the process would continue until the skyrmionium configuratiom is destroyed or until it turns to a domain wall extending to infinity in the x_2 direction.

IV. TRAVELING $Q = 1$ SKYRMION

Let us now consider topologically nontrivial solutions ($Q \neq 0$) such as the $Q = 1$ skyrmion of Fig. 1 which is a static solution of Eq. (1), and suddenly apply a spin-polarized current. In order to follow the skyrmion as it moves we will follow the coordinates of its guiding center (R_1,R_2) defined as the normalized moments in Eq. (10):

$$R_\mu = \frac{I_\mu}{4\pi Q} = \frac{1}{4\pi Q}\int x_\mu q\, d^2x. \tag{28}$$

They give a measure of the position of a skyrmion and are conserved quantities as explained in connection with Eqs. (10) and (9).

The instantaneous velocity $(\dot{R}_1,\dot{R}_2)$ is given through Eqs. (11). For the initial axially symmetric skyrmion solution of Eq. (1) we have $D_\mu = 0$ and $d_{12} = 0$, $d_{11} = d_{22} = W_{\rm ex}$, where $W_{\rm ex}$ is the exchange energy. Equation (11) gives

$$\dot{R}_1 = u\frac{1+\alpha\beta}{1+\alpha^2} = u + \frac{\alpha}{\bar{d}}\dot{R}_2, \quad \dot{R}_2 = u\frac{(\beta-\alpha)\,\bar{d}}{1+\alpha^2}, \tag{29}$$

where we denoted $\bar{d} = d_{11}/(4\pi Q) = d_{22}/(4\pi Q)$. Thus the skyrmion will initially have a velocity component in the direction of the current flow while its velocity component perpendicular to it depends on the sign of $\beta - \alpha$.

If we now assume that the skyrmion will eventually reach a propagating steady state then its velocity will satisfy the virial relations (16). For $Q \neq 0$ we define $\bar{d}_{\mu\nu} = d_{\mu\nu}/(4\pi Q)$ and write the virial relations as

$$\begin{aligned}(1-\alpha\bar{d}_{12})v_1 - \alpha\bar{d}_{22}v_2 &= (1-\beta\bar{d}_{12})u,\\ \alpha\bar{d}_{11}v_1 + (1+\alpha\bar{d}_{12})v_2 &= \beta u\,\bar{d}_{11}.\end{aligned} \tag{30}$$

These imply that, in general, both components of the velocity are nonzero, $v_1,v_2 \neq 0$; therefore, a propagating skyrmion will move at an angle to the flow of the spin current. Unlike in the case of a skyrmionium, dissipation is not necessary in order to obtain a steady state in the case of the skyrmion and Eqs. (30) give for $\alpha = 0$ the velocity

$$v_1 = u - \beta u\,\bar{d}_{12}, \quad v_2 = \beta u\,\bar{d}_{11}. \tag{31}$$

In order to obtain more detailed information on the propagating skyrmion configuration we study the case $\beta = \alpha$ since it emerges again as a special case as seen in Eq. (29). In a steady state Eq. (30) gives for the skyrmion a velocity $(v_1,v_2) = (u,0)$ collinear with the spin current. When we substitute this in Eq. (14) we obtain the static LL equation $\boldsymbol{m} \times \boldsymbol{f} = 0$. Thus the argument employed in Sec. III for a skyrmionium also applies for a skyrmion: a static skyrmion solution of the conservative LL Eq. (1), which we denote $\boldsymbol{n}(x_1,x_2)$, is a traveling solution of the full equation (4) with $\boldsymbol{m}(x_1,x_2,t) = \boldsymbol{n}(\xi_1,x_2)$ and $\xi_1 = x_1 - ut$.

It is well known that there are no traveling skyrmion solutions of Eq. (1), i.e., there are no $Q \neq 0$ skyrmion solutions of Eq. (23), and this can be rigorously established [26]. Therefore, the arguments about traveling skyrmionium solutions following Eq. (23) cannot be applied in the case of skyrmions.

For $\beta \neq \alpha$ a traveling skyrmion should have $v_2 \neq 0$ as shown by Eq. (30), that is, the skyrmion travels at an angle with respect to the direction of the flow of the spin current. In the case $\beta \neq \alpha$ we could not find exact traveling wave solutions of Eq. (4), for the effective field (2). Exact results are though indeed obtained for the pure exchange model in the Appendix.

For small deviations from the simple case $\beta = \alpha$ and $(v_1,v_2) = (u,0)$ we may assume that the skyrmion retains approximately axial symmetry, and thus we have a diagonal $\bar{d}_{\mu\nu} = \bar{d}\,\delta_{\mu\nu}$, where $\bar{d}$ is a constant. Equations (30) have now a relatively simple solution:

$$v_1 = u\frac{1+\alpha\beta\bar{d}^2}{1+(\alpha\bar{d})^2} = u + \alpha\bar{d}\,v_2, \quad v_2 = u\frac{(\beta-\alpha)\,\bar{d}}{1+(\alpha\bar{d})^2}. \tag{32}$$

For the pure exchange model $\bar{d} = 1$ (see the Appendix), while for other models such as in Eq. (2) we have $\bar{d} > 1$ calculated by substituting the static skyrmion solution of Eq. (1) in Eq. (12). Equation (32) gives the so-called mobility relation, i.e., a linear relation between the velocity and the current.

In order to check the theoretical predictions we have conducted a numerical simulation using the parameter set

$$\alpha = 0.2, \quad u = 0.1, \quad \beta = 0.5, \tag{33}$$

with large values for α,β and $\beta - \alpha$. We use as an initial condition the skyrmion of Fig. 1 with $\kappa = 3$ and apply the spin current. The numerically found velocity for the skyrmion

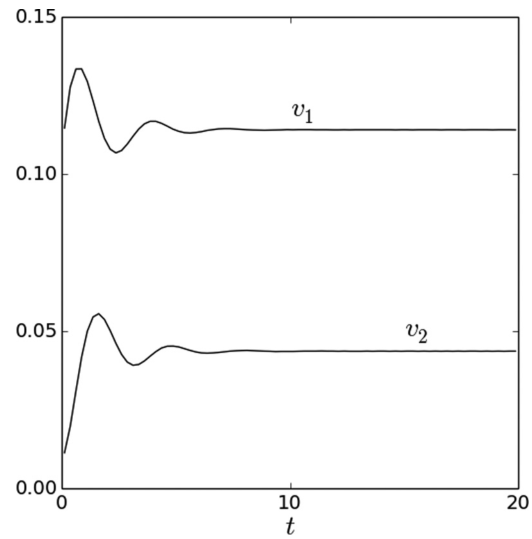

FIG. 5. Simulation results for the velocity components $(v_1,v_2) = \dot{R}_1,\dot{R}_2$ as a function of time t for a skyrmion under spin torque with parameter values (33).

is shown in Fig. 5. We initially have $\dot{R}_1 = 0.106$, $\dot{R}_2 = 0.044$; the velocity presents oscillations and eventually converges to constant values $(v_1,v_2) = (0.1140,0.0436)$. The expected initial velocity is found from Eqs. (29) and it is $\dot{R}_1 = 0.106$, $\dot{R}_2 = 0.046$, where we have used the numerically calculated value for the exchange energy $W_{\rm ex} = 20.08 \Rightarrow \bar{d} = 1.598$. The final velocity is in excellent agreement with the velocity at a steady state predicted by Eq. (32) which gives $(v_1,v_2) = (0.1139,0.0435)$, where we assume that the initial skyrmion profile is not significantly changed. The skyrmion configuration is indeed not visibly distorted during the simulation compared to the initial axially symmetric skyrmion.

We have also conducted a numerical simulation using the parameter set (27) and the results are again in excellent agreement with the predictions of Eqs. (29) and (32).

We finally note that the skyrmion is pinned at its final position when the spin current is switched off. This is contrasted with the dynamics of a skyrmionium which travels at a constant velocity also in the absence of external forces (and damping).

V. CONCLUDING REMARKS

We have studied the dynamics under spin torque of nontopological ($Q = 0$) and topological ($Q \neq 0$) skyrmions in films of Dzyaloshinskii-Moriya materials with easy-axis anisotropy. Analytical results are obtained using the equations for the linear momentum (for $Q = 0$) or the guiding center (for $Q \neq 0$), and virial relations. The study is complemented by a set of numerical simulations. Furthermore, we obtain exact solutions of the Landau-Lifshitz equation including spin torques, given in Eq. (4), for some particular cases. The traveling solutions obtained provide arguments that a spin polarized current will cause rigid motion of a skyrmion or a skyrmionium. This result is applicable not only for the solitons studied in the present work but also for other models, e.g., for driven motion of magnetic bubbles.

The $Q = 0$ skyrmionium is accelerated by the spin torque and it continues moving after switching off the current. This Newtonian dynamics was also observed in the case of the skyrmionium under an external field gradient [19]. It is dramatically different than the more well-studied dynamics of a skyrmion [12,15,16], which is spontaneously pinned in the absence of external torques. On the other hand, the skyrmionium motion presents some similarities with the skyrmion motion in a stripe geometry [16].

Model (1) has more solutions, beyond the skyrmion and the skyrmionium studied in the present paper. Axially symmetric static solutions exist where Θ in Eq. (7) takes the values $n\pi$, with n an integer, at spatial infinity: $\theta(\rho \to \infty) = n\pi$ [8]. Their dynamical properties depend crucially on their skyrmion number as our results, by example of the skyrmion and the skyrmionium, have shown. The skyrmion number of an $n\pi$-skyrmion is easily found to be $Q = 0$ for n even and $Q = 1$ for n odd [19]. The formal discussion for the dynamics of a skyrmion in Sec. IV remains valid for all $n\pi$-skyrmions with $Q = 1$, while those with $Q = 0$ should follow the dynamics discussed for a skyrmionium in Sec. III.

Our methods can be also applied to simpler one-dimensional models (wires) provided static domain wall solutions of Eq. (1) exist.

APPENDIX: PURE EXCHANGE MODEL

If we set $\boldsymbol{f} = \Delta \boldsymbol{m}$ we have the so-called pure exchange model and we will present analytic results which elucidate the discussion in Sec. IV. In the pure exchange model the Bogomol'nyi relations [30,31]

$$\partial_1 \boldsymbol{m} = \boldsymbol{m} \times \partial_2 \boldsymbol{m}, \quad \partial_2 \boldsymbol{m} = -\boldsymbol{m} \times \partial_1 \boldsymbol{m}, \tag{A1}$$

which contain only first order derivatives, are sufficient for obtaining static solutions of Eq. (1), i.e., solutions for $\boldsymbol{m} \times \boldsymbol{f} = 0$. A large class of $Q \neq 0$ skyrmion solutions can be found by solving (A1). Of those, the axially symmetric $Q = 1$ skyrmion configuration of the form (7) will be denoted $\boldsymbol{m} = \boldsymbol{n}(x_1,x_2)$ and reads

$$n_1 = -\frac{2ax_2}{\rho^2 + a^2}, \quad n_2 = \frac{2ax_1}{\rho^2 + a^2}, \quad n_3 = \frac{\rho^2 - a^2}{\rho^2 + a^2}, \tag{A2}$$

where a is a arbitrary positive constant giving the skyrmion radius and $\rho^2 = x_1^2 + x_2^2$. Configuration (A2) is similar in its gross features to that shown in Fig. 1.

We turn to Eq. (14) for a traveling steady state with velocity (υ_1,υ_2) and we require

$$\begin{cases} u - \upsilon_1 = -\alpha \upsilon_2 \\ \upsilon_2 = \beta u - \alpha \upsilon_1 \end{cases} \Rightarrow \begin{cases} \upsilon_1 = \frac{1+\alpha\beta}{1+\alpha^2}\, u, \\ \upsilon_2 = \frac{\beta-\alpha}{1+\alpha^2}\, u. \end{cases} \tag{A3}$$

Then, Eq. (14) simplifies to

$$(\alpha \upsilon_2\, \partial_1 + \upsilon_2 \partial_2)\boldsymbol{m} = \boldsymbol{m} \times \boldsymbol{f} + \boldsymbol{m} \times (\alpha \upsilon_2 \partial_2 - \upsilon_2\, \partial_1)\boldsymbol{m}. \tag{A4}$$

Under the Bogomol'nyi relations (A1) the terms on the left-hand side cancel with the last terms on the right-hand side, which originate in the damping and the nonadiabatic spin torque. Since the same Bogomol'nyi relations are sufficient for the vanishing of the first term on the right-hand side, we conclude that relations (A1) are sufficient conditions for solutions of Eq. (A4).

Therefore, any solution $\boldsymbol{m} = \boldsymbol{n}(x_1,x_2)$ of Eqs. (A1), such as the skyrmion in Eq. (A2), is a traveling solution $\boldsymbol{m}(x_1,x_2,t) = \boldsymbol{n}(\xi_1,\xi_2)$ of the full Eq. (4) with spin current and damping, with a velocity given by Eq. (A3).

Regarding calculations presented in Sec. IV it is useful to note that skyrmion solutions with $Q \neq 0$ which satisfy (A1) have exchange energy $W_{\text{ex}} = 4\pi Q$ [31]. Thus, for axially symmetric skyrmions, such as (A2), the tensor $d_{\mu\nu}$, defined in Eq. (12), is diagonal with $\bar{d}_{\mu\nu} = \delta_{\mu\nu}$. We then see that the velocity in Eq. (A3) coincides with that given in Eq. (32) applied for $\bar{d} = 1$.

[1] A. N. Bogdanov and D. A. Yablonskii, Zh. Eksp. Teor. Fiz. **95**, 178 (1989) [Sov. Phys. JETP **68**, 101 (1989)].

[2] A. N. Bogdanov and A. Hubert, J. Magn. Magn. Mater. **138**, 255 (1994).

[3] N. Romming, C. Hanneken, M. Menzel, J. E. Bickel, B. Wolter, K. von Bergmann, A. Kubetzka, and R. Wiesendanger, Science **341**, 636 (2013).

[4] N. Romming, A. Kubetzka, C. Hanneken, K. von Bergmann, and R. Wiesendanger, Phys. Rev. Lett. **114**, 177203 (2015).

[5] S. Mühlbauer, F. Binz, B. Jonietz, C. Pfleiderer, A. Rosch, A. Neubauer, R. Georgii, and P. Böni, Science **323**, 915 (2009).

[6] X. Z. Yu, Y. Onose, N. Kanazawa, J. H. Park, J. H. Han, Y. Matsui, N. Nagaosa, and Y. Tokura, Nature (London) **465**, 901 (2010).

[7] X. Z. Yu, N. Kanazawa, Y. Onose, K. Kimoto, W. Z. Zhang, S. Isiwata, Y. Matsui, and Y. Tokura, Nat. Mater. **10**, 106 (2011).

[8] A. N. Bogdanov and A. Hubert, J. Magn. Magn. Mater. **195**, 182 (1999).

[9] A. Leonov, U. K. Rößler, and M. Mostovoy, EPJ Web Conf. **75**, 05002 (2013).

[10] D. A. Allwood, G. Xiong, C. C. Faulkner, D. Atkinson, D. Petit, and R. P. Cowburn, Science **309**, 1688 (2005).

[11] K. Everschor, M. Garst, B. Binz, F. Jonietz, S. Mühlbauer, C. Pfleiderer, and A. Rosch, Phys. Rev. B **86**, 054432 (2012).

[12] A. Fert, V. Cros, and J. Sampaio, Nat. Nanotechnol. **8**, 152 (2013).

[13] J. Sampaio, C. Vincent, S. Rohart, A. Thiaville, and A. Fert, Nat. Nanotechnol. **8**, 839 (2013).

[14] N. Nagaosa and Y. Tokura, Nat. Nanotechnol. **8**, 899 (2013).

[15] J. Iwasaki, M. Mochizuki, and N. Nagaosa, Nat. Commun. **4**, 1463 (2013).

[16] J. Iwasaki, M. Mochizuki, and N. Nagaosa, Nat. Nanotechnol. **8**, 742 (2013).

[17] C. Schütte, J. Iwasaki, A. Rosch, and N. Nagaosa, Phys. Rev. B **90**, 174434 (2014).

[18] R. Tomasello, E. Martinez, R. Zivieri, L. Torres, M. Carpentieri, and G. Finocchio, Sci. Rep. **4**, 6784 (2014).

[19] S. Komineas and N. Papanicolaou, Phys. Rev. B **92**, 064412 (2015).

[20] M. Beg, D. Chernyshenko, M.-A. Bisotti, W. Wang, M. Albert, R. L. Stamps, and H. Fangohr, Sci. Rep. (to be published) [arXiv:1312.7665].

[21] N. S. Kiselev, A. N. Bogdanov, R. Schäfer, and U. K. Rößler, J. Phys. D **44**, 392001 (2011).

[22] J. C. Slonczewski, J. Magn. Magn. Mater. **159**, L1 (1996).

[23] L. Berger, Phys. Rev. B **54**, 9353 (1996).

[24] S. Zhang and Z. Li, Phys. Rev. Lett. **93**, 127204 (2004).

[25] M. Finazzi, M. Savoini, A. R. Khorsand, A. Tsukamoto, A. Itoh, L. Duò, A. Kirilyuk, T. Rasing, and M. Ezawa, Phys. Rev. Lett. **110**, 177205 (2013).

[26] N. Papanicolaou and T. N. Tomaras, Nucl. Phys. B **360**, 425 (1991).

[27] S. Komineas and N. Papanicolaou, Physica D **99**, 81 (1996).

[28] J. He, Z. Li, and S. Zhang, Phys. Rev. B **73**, 184408 (2006).

[29] K. Everschor, M. Garst, R. A. Duine, and A. Rosch, Phys. Rev. B **84**, 064401 (2011).

[30] A. A. Belavin and A. M. Polyakov, JETP Lett. **22**, 245 (1975).

[31] R. Rajaraman, *Solitons and Instantons* (North-Holland, Amsterdam, 1982).